Available online at www.sciencedirect.com
ScienceDirect
Trans. Nonferrous Met. Soc. China 34(2024) 1226−1236
Transactions of Nonferrous Metals Society of China
www.tnmsc.cn

Thermal insulation capability and adhesion strength of unpyrolyzed thick thermal barrier coatings

Mohammad IZADINIA[1,2], Reza SOLTANI[1], Mahmoud HEYDARZADEH SOHI[1], Javad MOSTAGHIMI[2]

1. School of Metallurgy and Materials Engineering, College of Engineering, University of Tehran, Tehran, Iran;
2. Centre for Advanced Coating Technologies, Department of Mechanical and Industrial Engineering, University of Toronto, Toronto, Ontario, Canada

Received 5 October 2022; accepted 8 June 2023

Abstract: Thermal insulation capability and adhesion strength of thick thermal barrier coatings (TBC) produced by unpyrolyzed powder (UPTTBC) were compared with those of the conventional TBC, thick TBC (TTBC), and dense vertically cracked (DVC) TTBC. Thermal insulation capability was evaluated using temperature drop. The adhesion strengths of the coatings were also measured by pull-off test method according to ASTM C633. The results indicated that the adhesion strength of UPTTBC and DVC TTBC was 35% and 25% higher than that of the TTBC, respectively. This could imply that the non-melted areas with sub-micron dimensions in UPTTBC structure, act as a trap and prevent the cracks propagation. In addition, the results of thermal insulation tests showed that DVC TTBC coatings had the lowest thermal insulation capability with temperature drop rate of 0.28 °C/μm and UPTTBC coatings had the highest insulation capability with temperature drop rate of 0.40 °C/μm. Due to the presence of sub-micron zones in the microstructure of UPTTBCs, the coatings exhibited superior thermal insulation capability. In contrary, the DVC TTBC showed the lowest thermal insulation capability because of its dense structure.

Key words: thick thermal barrier coating; dense vertically cracked thermal barrier coating; unpyrolyzed powder; adhesion strength; thermal insulation capability

1 Introduction

Thermal barrier coatings (TBCs), due to their low thermal conductivity, are widely used in gas turbines at high temperatures to reduce the surface temperature of hot section components. In fact, thermal barrier coatings by creating a temperature gradient, reduce the temperature of the substrate which results in higher engine efficiency and longer life of turbine components. To increase the efficiency of the engine, it is necessary to increase the working temperature, while the materials used in the engine have a temperature limit. Therefore, scientists are looking for improving the characteristics of the coating so that it can provide a higher temperature gradient [1−4].

The employing of thicker thermal barrier coatings (TTBCs) reduces the substrate temperature further and as a result, can increase the turbine inlet temperature of the engines and lowering the amounts of air needed for cooling hot section components. This will result in higher efficiencies of the engines. Despite better thermal insulation, increasing the thickness of TBCs reduces the service life of the coating [5,6]. Two main factors work simultaneously to reduce the service life of thick thermal barrier coatings: first, the higher the thermal gradient during service, the higher thermal stresses through the coating, and second, the elastic strain energy increase causing crack propagation in the coating [7].

Corresponding author: Reza SOLTANI, E-mail: rsoltani@ut.ac.ir
DOI: 10.1016/S1003-6326(24)66466-6

Many researches have been conducted to extend the service life of TTBCs by improving their microstructure; among them the formation of vertical cracks through the ceramic top coat has been very promising. Vertical cracks enhance the strain tolerance of the TTBCs and thus, the thermal stresses and thermal expansion mismatches between the bond coat and top coat are remarkably reduced. The dense vertically cracked (DVC) TBCs have been developed by increasing the density more than 85% in air plasma sprayed (APS) TBCs which is obtained by "hot spraying" [8]. As a result of the dense structure, inter-splat gaps and horizontal cracks are almost eliminated, which leads to an increase in the thermal conductivity of DVC TBCs [9−11].

The authors have published the results of the successful development of the unpyrolyzed thick thermal barrier coatings (UPTTBCs) produced by the APS method, elsewhere [12−14]. These coatings have vertical cracks which are formed due to the shrinkage induced from the pyrolysis process of un-melted particles and not from high density of the coating, and therefore they have moderate porosity. Since other studies have been focused on producing DVC TBCs which results in higher thermal conductivity [7,15], production of UPTTBCs will be a promising approach to reduce thermal conductivity of vertically cracked TBCs.

In addition to the other requirements of TBC systems, the adhesion strength is a main necessity of the coatings, as well. The capability of coating to adhere to the substrate during coating is called adhesion strength which is one of the most effective parameters in coatings quality. In the case of UPTTBCs, the residual stresses and submicron size zones throughout the coatings can affect the adhesion strength of the coatings. Generally, there are three bonding types, consisting of mechanical, physical, and metallurgical ones which can occur in thermal spray coatings. Several factors are at work which affect the bonding type like substrate and coating composition, surface temperature and roughness, kinetic energy, and temperature of the particles reached to the surface [16].

Cohesion and/or adhesion strength of thermal spray coatings are affected by adhesion of the melted and/or semi-melted particles to the substrate, splats morphology, strength between splats, morphology and size of cracks, porosities, and defects; the greater the adhesion/cohesion of the coating, the better the performance and the higher the life during service [17]. Since the UPTTBCs show bimodal microstructure with un-melted zones, there is a concern about the bonding of the adhesion and/or cohesion strength of the coating.

In the present study, the thermal insulation capability and adhesion strength of the UPTTBC have been evaluated and compared with the conventional TBC, TTBC, and DVC TTBC.

2 Experimental

2.1 Plasma spray process and sample characterization

The disc-shaped specimens with 25 mm in diameter and 2 mm in thickness were laser cut from Hastelloy X solid solution nickel-based superalloy and were used as substrate. In order to form the bond coat for all the specimens, Ni23Co17Cr12-Al0.5Y (wt.%) (Amdry 365-2, Oerlikon Metco) powder was used, and to form the top coat, agglomerated and sintered 7 wt.% yttria stabilized zirconia (7YSZ) (Amperit 827, Starck) was used for the TBC, TTBC, and DVC TTBC samples. The unpyrolyzed YSZ powder with the same chemical composition of Amperit 827 (7 wt.% yttria stabilized zirconia) was synthesized by the co-precipitation method using the appropriate ratio of zirconium oxynitrate and yttrium nitrate and was used to produce UPTTBCs. Before applying the bond coat, the substrate was grit blasted with alumina particles with 24 mesh, impact angle of 90°, at a pressure of 0.3−0.4 MPa and a distance of about 10 cm, in order to remove contaminations and surface oxides and make a rough surface. Argon gas was used as the carrier and primary gas and hydrogen were used as the secondary gas. Parameters of air plasma spraying which were applied by the 3MB gun are given in Table 1.

Scanning electron microscopy (SEM) (CamScan−MV2300) was used to evaluate the microstructures and chemical composition of the phases. Moreover, in order to achieve better evaluation, field emission SEM (Hitachi, SU 8040) was employed for fractography.

2.2 Adhesion strength test

ASTM C633 — 01 standard test method was used to determine adhesion strength (bonding strength) of a coating to a substrate or the cohesion

Table 1 Parameters of air plasma spraying

Sample	Primary gas flow rate/(L·min^{-1})	Secondary gas flow rate/(L·min^{-1})	Current/A	Gun speed/(m·s^{-1})	Feeding rate/(r·min^{-1})	Distance/cm
Bond	55	14	700	0.7	3	12
Conventional TBC	46	14	700	0.9	6	12
TTBC	48	12	700	1	4	10
UPTTBC	48	12	700	1	2.5	10
DVC TTBC	46	14	700	0.6	6	7

strength of the coating [18]. According to this standard, if the fracture occurs at the top coat/bond coat interface or the bond coat/substrate interface, the value is called adhesion; if the fracture occurs within the top coat or the bond coat, it shows the cohesion strength of the coating [19−22].

2.3 Thermal insulation test

The thermal insulation capability was evaluated using temperature drop across the coating with a system designed, as shown in Fig. 1. Furnace temperature T_0, the temperature of reference sample T_1, and temperature of the sample with thermal barrier coating T_2 are defined. The temperature was recorded during the test and temperature versus time curve was plotted. At about 10 min after the furnace temperature was reached to 1200 °C, T_1 and T_2 became fixed and then the thermal insulation capability was obtained by the mean value of temperature reduction across the coating ($\Delta T=T_1-T_2$). Figure 1 shows thermal insulation test schematically.

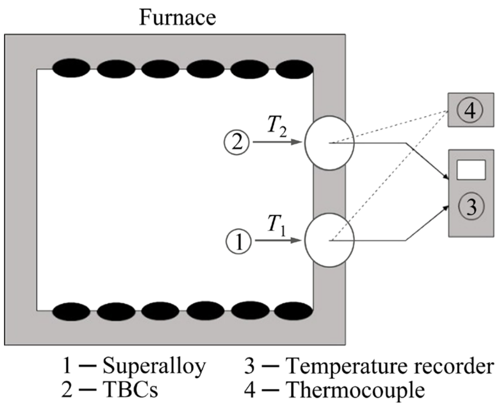

Fig. 1 Schematic representation of thermal insulation test

3 Results and discussion

3.1 Microstructure of coatings

Figure 2 illustrates morphology and microstructure of the unpyrolyzed powder produced by co-precipitation method.

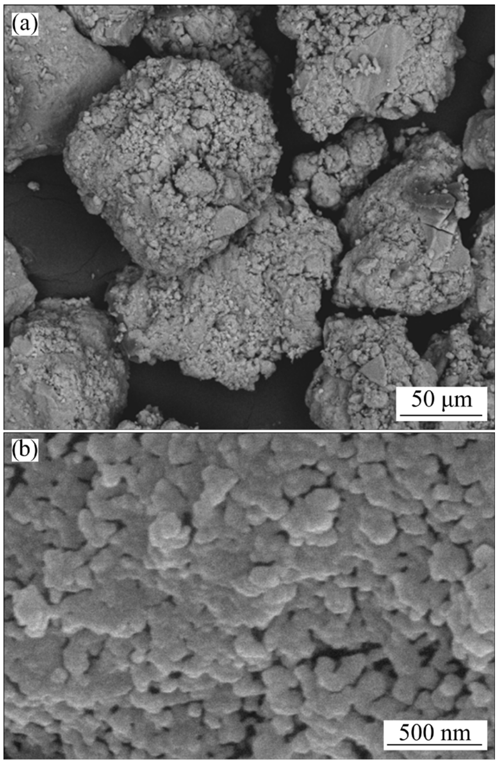

Fig. 2 SEM images of unpyrolyzed powder

Figure 3 shows the cross-sectional micrograph of conventional and thick TBCs deposited with parameters given in Table 1. The bond coat consists of splats separated by oxidized boundaries with a thickness of (210±10) μm. Top coats have the typical structure of TBCs including splats and porosities; the thicknesses for conventional TBC and TTBC samples are measured to be (491±28) and (920±21) μm, respectively. The average value of thicknesses was achieved by Image Analysis Software after ten measurements.

Decreasing the spraying distance and the plasma gun speed, in the deposited samples of DVC TTBC, as shown in Table 1, results in the formation of vertical cracks in the coating. Figure 4 shows a dense structure along vertical cracks across the top coat. Shrinkage of solidification as well as inter-splat bonding during deposition result in an

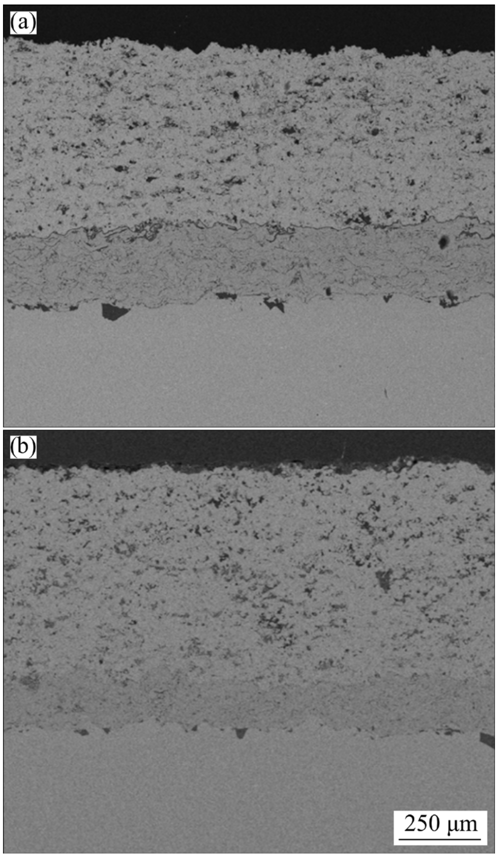

Fig. 3 Cross sectional microstructure of conventional TBC (a) and TTBC (b) produced under condition of Table 1

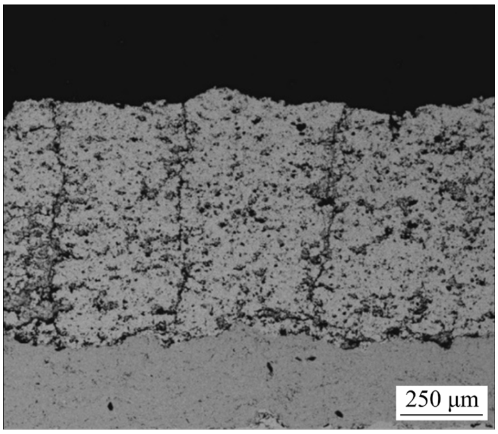

Fig. 4 Cross sectional image of DVC TTBC

increase in tensile stresses which when released cause the formation of vertical cracks [23−25]. When the length of vertical cracks is more than half of the coating thickness, they are called segmentation cracks. Moreover, the density of segmentation cracks (D_s) is defined as the number of segmentation cracks against the coating length. D_s is obtained to be 2.9 mm^{-1}, according to measurement of 5 images of the sample. In the present work, in order to obtain DVC structure, spray distance, gun speed, and argon/hydrogen gas flow rates ratio are reduced, as shown in Table 1.

Figure 5(a) shows the bimodal microstructure of the UPTTBC sample in which semi and/or non-molten submicron-sized particles are trapped among conventional splats (some semi and/or non-molten zones are marked by a white arrow in the structure). Vertical cracks are also observed in the structure, which distinguishes these coatings from conventional bimodal coatings produced by using nanostructured powders that have been studied in previous researches [14,26−28]. In order to achieve a bimodal structure in the UPTTBC coatings, the melting of un-pyrolyzed agglomerated powders during the spraying process is controlled in such a way that the outer shell of the particle is melted and the particle core remains intact. Figure 5(b) shows non-molten particles surrounded by normal splats. By controlling particles melting, the molten part acts as a binder, and the final structure is formed of semi and/or non-molten particles that are trapped within the typical splats.

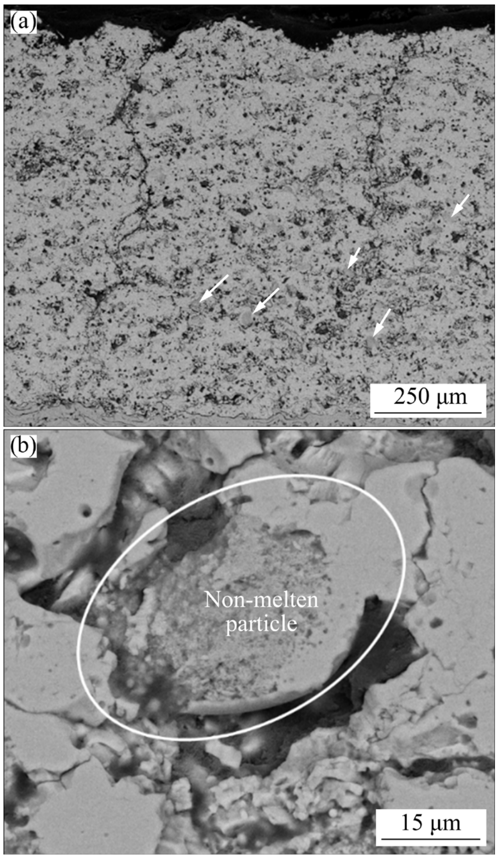

Fig. 5 Cross sectional SEM images of UPTTBC (a) and non-molten particles (b)

However, a remarkable feature of the coating produced with unpyrolyzed powder is the formation of vertical cracks in the coating structure which is not normally observed in bimodal coatings. The D_s values for the UPTTBC was measured to be 2.1 mm^{-1}.

Figure 6(a) shows the fracture surface of the UPTTBC sample in which microporosity, intra and inter splat cracks can be observed in the structure. In higher magnification (Fig. 6(b)), the bimodal structure can be seen, as well, including fully melted and solidified particles along with semi-melted ones. Also, some spherical particles can be seen in the microstructure.

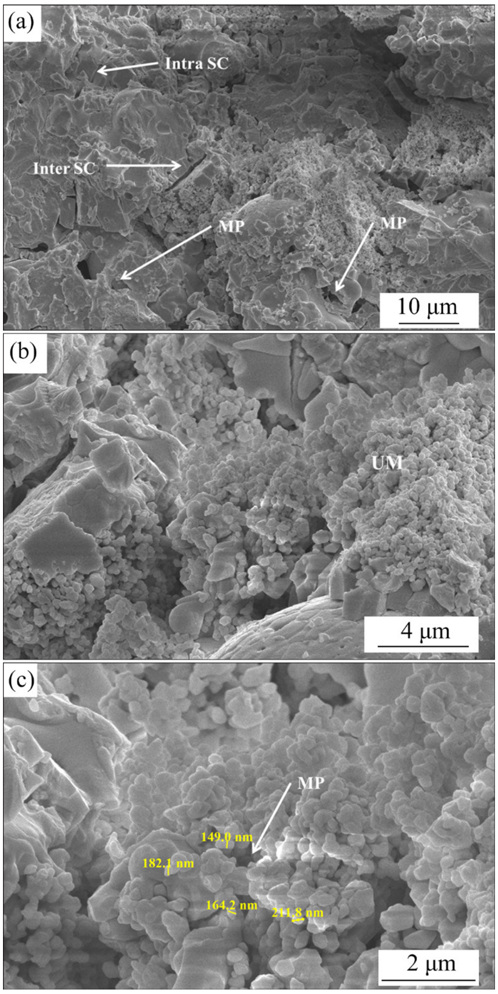

Fig. 6 FESEM surface fracture micrographs of UPTTBC (UM: Remnant un-melted mass; MP: Micro-sized/submicron-sized pore; Inter SC: Inter splat crack; Intra SC: Intra splat crack; SP: Spherical particles)

Figure 6(c) illustrates nano/submicron-sized pores that exist within the remnant un-melted masses. This structure is formed when some unpyrolyzed particles cannot reach the appropriate temperature in the plasma plume for melting, and therefore are embedded in the coating as un-melted ones.

3.2 Adhesion strength

The results of adhesion strength tests for the conventional TBC, thick TBC, DVC TTBC, and UPTTBC are listed in Table 2. The average tensile strengths of the samples are shown in Fig. 7 for a better comparison. The stress−strain curve for all the samples showed no apparent plastic deformation before fracture, and thus, a brittle fracture occurred.

Table 2 Adhesion strength test results for TBC, TTBC, DVC TTBC and UPTTBC (MPa)

Sample	1	2	3	Average
Conventional TBC	26.1	24.3	28.6	26.3
TTBC	19.8	21.2	18.9	20
DVC TTBC	24.1	25.1	27.1	25.4
UPTTBC	28.7	30.1	24.1	27.6

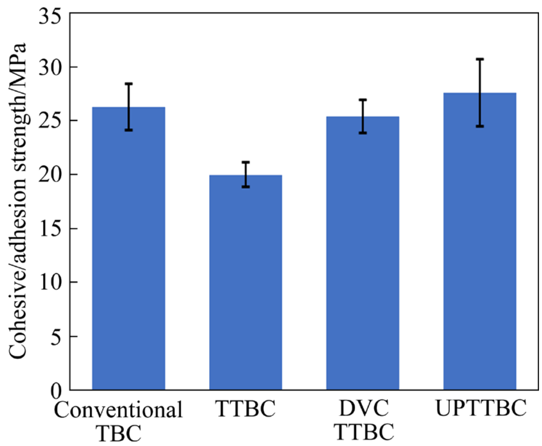

Fig. 7 Comparison of adhesion strength of different TBCs

Comparison of the adhesion strengths of conventional TBC and TTBC samples indicates that as the thickness of the coating increases, the adhesion strength of the top coat/bond coat decreases, which shows the dependency of the thickness and adhesion strength. As the thickness doubles, adhesion strength is reduced by approximately 25%. The increase of shrinkage forces resulting from thicker coating which acts against the bonding forces could be the reason for this drop in the strength value. STEFFENS et al [29] reported that with an increase of coating thickness of 7YSZ from 0.3 mm to over 4 mm, the adhesion strength decreases from 38 to 10 MPa. Another research by LEE et al [6] about the effects of different spray guns and the thickness of the ceramic coating on adhesion strength of TBC showed that the adhesion strength for the 600 μm TBCs was higher than that of 2000 μm-thick TBCs, independent of the spray gun; The adhesion strengths of TBCs with the thickness of 600 μm produced by 9MB and Triplex were (79±1.0) and (79±0.6) MPa, respectively, which proves the independency of the type of gun.

The DVC TTBC samples have higher adhesion strength compared to TTBC samples. In order to explain this behavior for DVC TTBC, adhesion mechanisms need to be evaluated. Generally, three types of bonding between the particles and the substrate are considered in thermal barrier coatings:

(1) Mechanical bonding: mechanical interlocking due to the surface roughness of the substrate (this roughness is formed by sandblasting of substrate before plasma spraying process or by depositing a bond coat before spraying the ceramic layer).

(2) Metallurgical bonding: chemical reactions on the surfaces due to diffusion.

(3) Epitaxial bonding between similar crystal structure of coating and substrate [30].

During spraying at low temperatures, mechanical interlocking would be the main adhesion mechanism. High-strength bonding occurs between the colliding particles and the substrate surface by the flow of molten droplets on the surface and their solidification around the irregularities of the surface. Shrinkage due to rapid cooling of sprayed particles increases the adhesion strength caused by mechanical interlocks. The high temperature of the substrate during spraying may cause metallurgical bonding between splats and substrate. If the sprayed material had a crystal structure similar to or the same as that of the substrate, an epitaxy mechanism could be added, as well [31].

Therefore, two types of bonding may be involved in the desired adhesion strength of dense TBC: (1) mechanical and (2) chemical. If the temperature of the molten particles, reaching the surface, is high enough, the possibility of splats break up, the splashing of the particles after hitting the surface decreases and the splats tend to flatten into a disc shape [32,33]. FUKUMOTO et al [34] showed that at high rates of cooling of molten particles on the substrate, a porous solidified layer is formed at the contact surface of the particle and the substrate, which accelerates the rate of molten droplet expansion and splashing; while at lower solidification rates, a better bond between splats and substrates is formed and splat flattening is dominated, which causes the formation of disc-shaped splats. According to Rayleigh–Taylor instability, the more rapidly the droplet flattens, the more complex the shape of droplet is, i.e. splashing occurs [34].

Molten particles splashing, after hitting the surface, leads to cavities in the joint of the substrate and the coating. These cavities can be too small to be filled with subsequent splats, which may cause cooling to occur more rapidly, which reduces the time for chemical bonding [35].

Therefore, in the case of the DVC TTBC sample, due to the higher temperature of the particles that reach the surface, solidification in the form of a disc is encouraged, which creates a stronger mechanical bond and a longer solidification time, thus providing the conditions for chemical bonding. In addition to the mentioned factors, it should be noted that in thermal barrier coatings with vertical cracks, the stresses caused by the contraction of the splats are released as a result of the growth of vertical cracks. Therefore, the residual stresses in the coating structure which resist against the mechanical and chemical bonding of the coating and substrate decrease.

By comparing the adhesion strength of UPTTBC with TTBC and DVC TTBC, it was found that the adhesion of UPTTBC is stronger than TTBC and DVC TTBC. As observed in the microstructure evaluation, this coating contains areas of un-melted powders with sub-micron size particles. Although these areas reduce the hardness of the coating, they can act as areas resistant to the growth of micro-cracks and prevent the destruction of the coating under tensile stresses. LIMA and MARPLE [36] compared the adhesion strength of micrometer and sub-micrometer titanium oxide (TiO_2) coatings produced by thermal spraying and found that coatings with sub-micrometer areas have higher adhesion strength. BANSAL et al [37] compared the inter-facial toughness in conventional and bimodal (nanostructured) plasma spraying coatings of Al_2O_3−13wt.%TiO_2. They found that in the interface of the substrate and the first fully molten splats in both coatings, cracks occurred, whereas the partially molten regions in nano-coatings were completely adherent. Therefore, another factor, for having higher adhesion strength of the UPTTBC, could be the proper adhesion of partially molten sub-micrometer particles to the substrate.

Images of specimens after the adhesion test, including conventional thermal barrier coating, thick thermal barrier coating, thick thermal barrier coating with dense vertical cracks, and thermal barrier using unpyrolyzed powder are shown in Fig. 8.

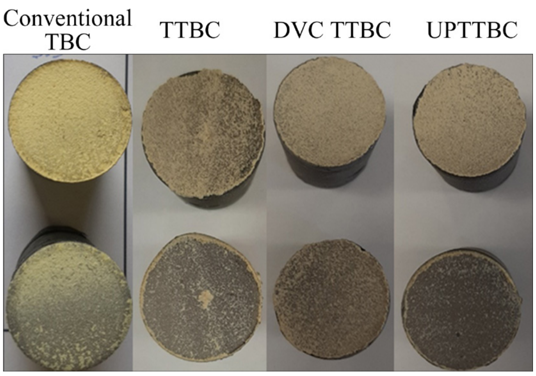

Fig. 8 Images of specimens after adhesion test

According to Fig. 8, almost in none of the adhesive strength tests, coatings were detached completely from the interface of the substrate and the bond coat. SMITH et al [38] showed that the adhesion of the bond coat to the substrate in thermal barrier coatings is usually adequate and is higher than 40 MPa. Moreover, in thermal barrier coatings, the adhesion of the bond coat and the ceramic top layer is important and the coatings will fail in this area more probably. It should be noted that the bond coat has a crystal structure similar to the substrate and therefore the epitaxial adhesion mechanism, in addition to mechanical interlocks, helps to increase the adhesion strength of nickel-based splats to the nickel-based substrate and this adhesion is usually better than that of ceramic splats to the metallic ones. Besides, since the difference in thermal expansion coefficient (CTE) of the bond coat and the top layer is greater than the difference of CTE of the bond coat and substrate, the residual thermal stresses on the interface of the top and bond coat are more than those of the bond coat and substrate. Therefore, the interface of the top-bond coat is more prone to crack initiation and subsequent growth during the adhesion test [16].

3.3 Thermal insulation capability

The most important purpose of using thermal barrier coatings is to protect the substrate from high temperatures and reduce the operating temperature of the substrate. Therefore, thermal insulation can be one of the most important variables in evaluating thermal barrier coatings.

Figure 9 shows the thermal insulation diagram for the conventional TBC. According to the results, the average temperature drop for conventional coating was measured at about 188 °C.

Figure 10 shows the thermal insulation diagram for the TTBC sample. Based on the results, the average temperature drop for thick coating is about 338 °C. As can be seen, the amount of temperature drop depends on the thickness of the coating, and the thick thermal barrier coating with a thickness of 920 μm has further reduced the substrate temperature by 79% compared to the conventional one with 490 μm in thickness.

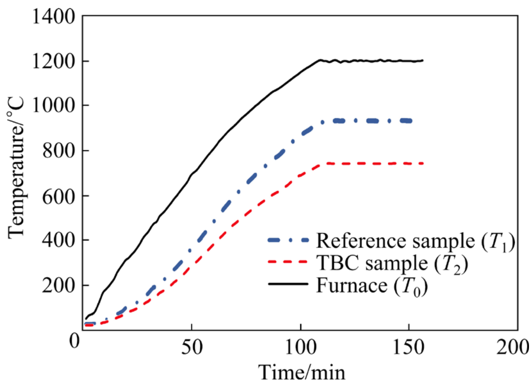

Fig. 9 Temperature−time diagram of furnace, reference sample and conventional TBC sample

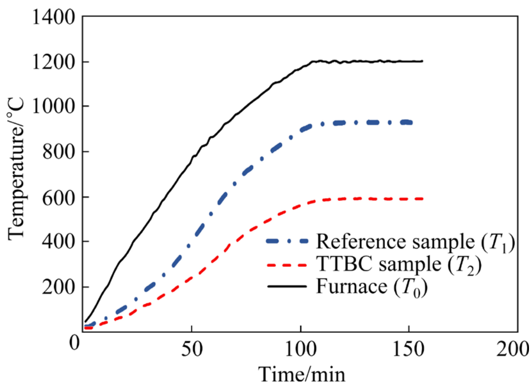

Fig. 10 Temperature−time diagram of furnace, reference sample and TTBC sample

Figure 11 shows the thermal insulation diagram for a thick thermal barrier with a dense structure. According to the results, the average temperature drop for the coating is about 232 °C. Thick thermal barrier coatings with dense structures compared to thick thermal barrier coatings show less ability to reduce the temperature of the substrate, which is due to the different structures of these coatings. In thermal barrier coatings, porosity and inter-splat cracks/gaps are the most important factors in reducing heat transfer. Since dense thermal barrier coatings have less porosity and also due to high spray temperature, the density of inter-splat boundaries have decreased, so heat transfer has increased.

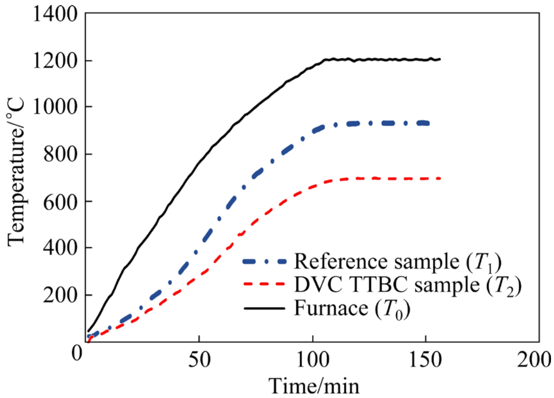

Fig. 11 Temperature−time diagram of furnace, reference sample and DVC TTBC sample

Figure 12 shows the thermal insulation diagram for the thick thermal barrier coating produced with unpyrolyzed powder. According to the diagram, the average temperature drop for the coating is about 370 °C. The thermal insulation capability of deposited thermal barrier coatings using unpyrolyzed powder is higher than that of the thick thermal barrier coatings and thick thermal barrier coatings with dense structure. Obviously, increasing the porosity of this coating compared to dense coatings is the main factor in increasing this capability, but comparing the results of thermal insulation capability of this coating with a thick thermal barrier coating that has almost the same porosity shows other factors are effective in this temperature drop. The microstructure of the coating with unpyrolyzed powder showed bimodal structure compared to the conventional coatings, which includes non-melted areas with sub-micrometer particles. These areas create more grain boundaries in the structure and these boundaries can cause phonon scattering.

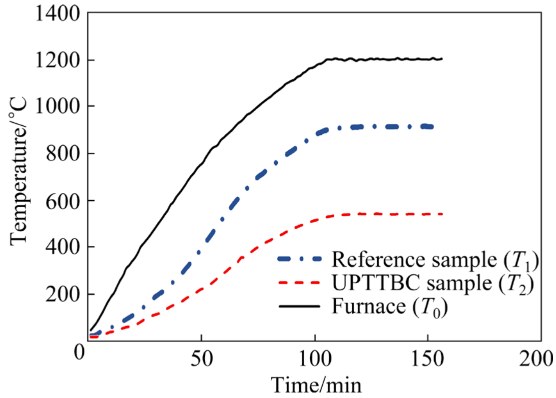

Fig. 12 Temperature−time diagram of furnace, reference sample and UPTTBC sample

Variables such as thickness, chemical composition, crystal structure and microstructure of the coating are effective in reducing the heat transfer of thermal barrier coatings [39].

(1) Thickness of the coating: Thermal barrier coatings are used in parts that have cooling, so the temperature gradient is created through the TBCs and with increasing the thickness of the coating, the temperature drop increases.

(2) Microstructure: The microstructure of thermal spraying coatings consists of splats and porosities and micro-cracks/gaps are created among the splats. The porosities and microcracks are in the perpendicular direction to the heat transfer direction and reduce the heat transfer in the coating [39].

(3) Crystal structure: Phonon scattering causes thermal insulation in TBCs. Therefore, the decrease in thermal conductivity is related to the phonon scattering. Phonon scattering reduces the phonon mean free path and reduces heat transfer. Phonon mean free path is affected by phonon−phonon scattering, scattering due to defects and grain boundaries. The phonon mean free path (l) is defined by Eq. (1) [40]:

$$\frac{1}{l}=\frac{1}{l_{\mathrm{i}}}+\frac{1}{l_{\mathrm{p}}}+\frac{1}{l_{\mathrm{gb}}} \tag{1}$$

where l_{i}, l_{p} and l_{gb} are defined as intrinsic scattering conductively, scattering due to point defects and scattering due to grain boundaries, respectively. The zirconia-based coatings have low intrinsic scattering conductively [40]. The degree of phonon scattering due to defects depends on the number of defects and their strength. The degree of strength is related to the quadratic difference between the atomic mass of the solute atom and the solvent atom. In the case of YSZ coatings, point defects due to the replacement of Zr with Y are negligible due to their low strength, as they have close atomic mass (yttrium 89 g/mol and zirconia 91 g/mol) [41]. Therefore, the vacancy has a greater effect than the substitutional atoms, and the reason for the decrease in heat transfer in these coatings is the creation of an O^{-2} vacancy, which is created by adding yttria to zirconia to balance the ionic network electrically. In conventional zirconia-based thermal barrier coatings, scattering due to grain boundary is negligible due to the short phonon mean free path compared to grain size [42].

The results of the thermal insulation capability of thermal barrier coatings are summarized in Table 3. In order to more accurately compare the effect of microstructure on heat transfer and avoid the effect of coating thickness on the results, the amount of temperature drop per 100 μm coating thickness (temperature drop rate) is reported.

Table 3 Temperature drops in thermal insulation capability test

Sample	Coating thickness/ μm	Temperature drop/°C	Temperature drop rate/ (°C·μm^{-1})
Conventional TBC	~491	188	0.38
TTBC	~920	338	0.37
DVC TTBC	~820	232	0.28
UPTTBC	~910	370	0.40

The results of thermal insulation test show that DVC TTBC coatings have the lowest and UPTTBC coatings have the highest thermal insulation capability. In this study, the influence of coating thickness, intrinsic heat transfers and point defects in the analysis of the results shown in Table 3 can be neglected, and thus the microstructure is the most important factor which affects the thermal insulation capability. Hot spraying in the case of the DVC TTBCs results in dense structure and reduction of porosity, which leads to the increase of heat transfer. Therefore, using DVC coatings, which have the advantage of high strain tolerance, could be less favorable due to the increased heat transfer [10].

In the case of UPTTBCs which have the best thermal insulation capability, it seems that, the presence of non-melted areas and sub-micron size porosity have reduced the heat transfer in the coating. RAUF et al [40] reported that small grain size can affect phonon scattering, so submicron-sized crystalline grains in non-melted areas of UPTTBCs can reduce heat transfer.

4 Conclusions

(1) Air plasma spraying the unpyrolyzed YSZ powder leads to the bimodal microstructure with columnar structure in the melted zone and the remaining un-melted submicron-sized particles along with vertical cracks throughout coating thickness.

(2) UPTTBCs have higher adhesion strength in comparison with the TTBCs and DVC TTBCs, since UPTTBCs contain submicron-zone and have the capability to control crack propagation.

(3) Thermal insulation in DVC TTBC coatings is severely reduced due to reduced porosity and elimination of inter-splat spaces. The presence of numerous porosities inside the submicron-sized zones and higher phonon scattering due to increased grain boundaries in splats improve the thermal insulation of the UPTTBCs, as compared with the conventional TTBCs.

CRediT authorship contribution statement

Mohammad IZADINIA: Investigation, Visualization, Formal analysis, Data curation, Writing − Original Draft; **Reza SOLTANI:** Corresponding author, Supervision, Project Administration, Conceptualization, Methodology, Editing; **Mahmoud HEYDARZADEH SOHI:** Supervision, Review, Editing; **Javad MOSTAGHIMI:** Review.

Declaration of competing interest

The authors declare that they have no known competing financial interests or personal relationships that could have appeared to influence the work reported in this paper.

References

[1] VOURDAS N, MARATHONITI E, PANDIS P K, ARGIRUSIS C, SOURKOUNI G, LEGROS C, MIRZA S, STATHOPOULOS V N. Evaluation of $LaAlO_3$ as top coat

material for thermal barrier coatings. [J]. Transactions of Nonferrous Metals Society of China, 2018, 28(8): 1582−1592.

[2] GONG S, CHEN M, HUANG X, ZHANG F. CMAS corrosion resistance characteristics of $RE_{50}Ta_xZr_{50-x}O_{175+0.5x}$ thermal barrier oxides in $RE_2Zr_2O_7$-$RETaO_4$ systems. [J]. Transactions of Nonferrous Metals Society of China, 2022, 32(12): 4014−4029.

[3] GIAMPAOLO T. Gas turbine handbook: Principles and practices [M]. 3rd ed. The Fairmont Press, Inc, 2007.

[4] SOLTANI R, COYLE T W, MOSTAGHIMI J. Microstructure and creep behavior of plasma-sprayed yttria stabilized zirconia thermal barrier coatings [J]. Journal of Thermal Spray Technology, 2008, 17(4): 244−253.

[5] MEHBOOB G, LIU M J, XU T, HUSSAIN S, MEHBOOB G, TAHIR A. A review on failure mechanism of thermal barrier coatings and strategies to extend their lifetime [J]. Ceramics International, 2020, 46(7): 8497−8521.

[6] LEE P H, LEE S Y, KWON J Y, MYOUNG S W, LEE J H, JUNG Y G, CHO H, PAIK U. Thermal cycling behavior and interfacial stability in thick thermal barrier coatings [J]. Surface and Coatings Technology, 2010, 205: 1250−1255.

[7] LU Z, KIM M S, MYOUNG S W, LEE J H, JUNG Y G, KIM I S, JO C Y. Thermal stability and mechanical properties of thick thermal barrier coatings with vertical type cracks [J]. Transactions of Nonferrous Metals Society of China, 2014, 24(Supplement 1): s29−s35.

[8] IZADINIA M, SOLTANI R, SOHI M H. Effect of segmented cracks on TGO growth and life of thick thermal barrier coating under isothermal oxidation conditions [J]. Ceramics International, 2019, 16(6): 7475−7481.

[9] QIU S, LIU Y C, GUO H, HUANG C G, MA Y, WU C W. Effect of splat-interface discontinuity on effective thermal conductivity of plasma sprayed thermal barrier coating [J]. Ceramics International, 2020, 46(4): 4824−4831.

[10] XIE L, CHEN D, JORDAN E H, OZTURK A, WU F, MA X, CETEGEN B M, GELL M. Formation of vertical cracks in solution-precursor plasma-sprayed thermal barrier coatings [J]. Surface and Coatings Technology, 2006, 201: 1058−1064.

[11] ZHAO H, YU F, BENNETT T D, WADLEY H N G. Morphology and thermal conductivity of Yttria-stabilized zirconia coatings [J]. Acta Materialia, 2006, 54(19): 5195−5207.

[12] IZADINIA M, SOLTANI R, SOHI M H, COYLE T. Effect of using unpyrolyzed powder on mechanical properties of vertically cracked thermal barrier coatings [J]. Surface and Coatings Technology, 2023, 459: 129404.

[13] IZADINIA M, SHAMANIAN M, MOHAMMADI H, KEYVANLOU H, NOURI A R. Improvement in the environmental resistance to oxidation and surface properties of simple carbon steel using aluminum coating [J]. Transactions of the Indian Institute of Metals, 2012, 65(5): 497−502.

[14] IZADINIA M, SOLTANI R, SOHI M H. Formation of vertical cracks in air plasma sprayed YSZ coatings using unpyrolyzed powder [J]. Ceramics International, 2020, 46(14): 22383−22390.

[15] MADHWAL M, JORDAN E H, GELL M. Failure mechanisms of dense vertically-cracked thermal barrier coatings [J]. Materials Science and Engineering A, 2004, 384(1/2): 151−161.

[16] LOGHMAN-ESTARKI M R, HAJIZADEH-OGHAZ M, EDRIS H, SHOJA RAZAVI R, GHASEMI R, VALEFI Z, JAMALI H. Plasma-sprayed nanostructured scandia−yttria and ceria−yttria codoped zirconia coatings: Microstructure, bonding strength and thermal insulation properties [J]. Ceramics International, 2018, 44(11): 12042–12047.

[17] ITO K, SHIMA T, FUJIOKA M, ARAI M. Improvement of oxidation resistance and adhesion strength of thermal barrier coating by grinding and grit-blasting treatments [J]. Journal of Thermal Spray Technology, 2020, 29(4): 1728–1740.

[18] ASTM C633—01. Standard test method for adhesion or cohesion strength of thermal spray coatings [S]. ASTM International, 2001.

[19] GHASEMI, R, VAKILIFARD H. Plasma-sprayed nanostructured YSZ thermal barrier coatings: Thermal insulation capability and adhesion strength [J]. Ceramics International, 2017, 43(12): 8556−8563.

[20] GHASEMI R, SHOJA-RAZAVI R, MOZAFARINIA R, JAMALI H. Comparison of microstructure and mechanical properties of plasma-sprayed nanostructured and conventional yttria stabilized zirconia thermal barrier coatings [J]. Ceramics International, 2013, 39(8): 8805−8813.

[21] SCHWEDA M, BECK T, OFFERMANN M, SINGHEISER L. Thermographic analysis and modelling of the delamination crack growth in a thermal barrier coating on Fecralloy substrate [J]. Surface and Coatings Technology, 2013, 217: 124−128.

[22] DOLEKER K M, KARAOGLANLI A C. Comparison of oxidation behavior of YSZ and $Gd_2Zr_2O_7$ thermal barrier coatings (TBCs) [J]. Surface and Coatings Technology, 2017, 318: 198−207.

[23] KARGER M, VAßEN R, STÖVER D. Atmospheric plasma sprayed thermal barrier coatings with high segmentation crack densities: Spraying process, microstructure and thermal cycling behavior [J]. Surface and Coatings Technology, 2011, 206: 16−23.

[24] GUO H B, VAßEN R, STÖVER D. Atmospheric plasma sprayed thick thermal barrier coatings with high segmentation crack density [J]. Surface and Coatings Technology, 2004, 186: 353−363.

[25] GUO H B, MURAKAMI H, KURODA S. Effect of hollow spherical powder size distribution on porosity and segmentation cracks in thermal barrier coatings [J]. Journal of the American Ceramic Society, 2006, 89(12): 3797−3804.

[26] ZENG S, ZHAO A, JIANG H. Oxidation of conventional and nanostructured 8 wt.% yttria-stabilized zirconia coating surface coatings on γ-TiAl [J]. Applied Surface Science, 2015, 332: 362–367.

[27] QAZI LAVASANI H, VALEFI Z, EHSANI N, TAMADDON MASOULE S. Comparison of the effect of sintering on the microstructure, micro hardness and phase composition of conventional and nanostructured YSZ TBCs [J]. Ceramics International, 2017, 43(15): 12497−12504.

[28] LOGHMAN-ESTARKI M R, SHOJA RAZAVI R, JAMALI H. Thermal stability and sintering behavior of plasma

sprayed nanostructured 7YSZ, 15YSZ and 5.5SYSZ coatings at elevated temperatures [J]. Ceramics International, 2016, 42(13): 14374−14383.

[29] STEFFENS H D, BABIAK Z, GRAMLICH M. Some aspects of thick thermal barrier coating lifetime prolongation [J]. Journal of Thermal Spray Technology, 1999, 8(4): 517−522.

[30] PAWLOWSKI L. The science and engineering of thermal spray coatings [M]. 2nd Edition. Chichester: Wiley, 2008.

[31] NIJDAM T J, MARIJNISSEN G H, VERGELDT E, KLOOSTERMAN A B, SLOOF W G. Development of a pre-oxidation treatment to improve the adhesion between thermal barrier coatings and NiCoCrAlY bond coatings [J]. Oxidation of Metals, 2006, 66(5/6): 269−294.

[32] FUKUMOTO M, TANAKA Y, NISHIOKA E. Flattening problem of thermal sprayed particles [J]. Materials Science Forum, 2004, 449/450/451/452: 1309−1312.

[33] WEI P, WEI Z, LI S, TAN C, DU J. Splat formation during plasma spraying for 8 mol.% Yttria-stabilized zirconia droplets impacting on stainless steel substrate [J]. Applied Surface Science, 2014, 321: 538−547.

[34] FUKUMOTO M, NISHIOKA E, MATSUBARA T. Flattening and solidification behavior of a metal droplet on a flat substrate surface held at various temperatures [J]. Surface and Coatings Technology, 1999, 120/121: 131−137.

[35] HEIMANN R B. Plasma- spray coating principles and applications [M]. 2nd ed. New York: VCH, 1996.

[36] LIMA R S, MARPLE B R. Enhanced ductility in thermally sprayed titania coating synthesized using a nanostructured feedstock [J]. Materials Science and Engineering A, 2005, 395(1/2): 269−280.

[37] BANSAL P, PADTURE N P, VASILIEV A. Improved interfacial mechanical properties of Al_2O_3−13wt.%TiO_2 plasma-sprayed coatings derived from nanocrystalline powders [J]. Acta Materialia, 2003, 51(10): 2959−2970.

[38] SMITH J, SCHEIBEL J, CLASSEN D, PASCHKE S, ELBEL S, FICK K, CARLSON D. Thermal barrier coating validation testing for industrial gas turbine combustion hardware [J]. Journal of Engineering for Gas Turbines and Power, 2016, 138(3): 1−7.

[39] WANG L, WANG Y, SUN X G, HE J Q, PAN Z Y, ZHOU Y, WU P L. Influence of pores on the thermal insulation behavior of thermal barrier coatings prepared by atmospheric plasma spray [J]. Materials and Design, 2011, 32(1): 36−47.

[40] RAUF A, YU Q, JIN L, ZHOU C. Microstructure and thermal properties of nanostructured lanthana-doped yttria-stabilized zirconia thermal barrier coatings by air plasma spraying [J]. Scripta Materialia, 2012, 66(2): 109−112.

[41] SONG X, XIE M, MU R, ZHOU F, JIA G, AN S. Influence of the partial substitution of Y_2O_3 with Ln_2O_3 (Ln=Nd, Sm, Gd) on the phase structure and thermophysical properties of ZrO_2−Nb_2O_5−Y_2O_3 ceramics [J]. Acta Materialia, 2011, 59(10): 3895−3902.

[42] GUO L, LI M, YE F. Phase stability and thermal conductivity of RE_2O_3 (RE=La, Nd, Gd, Yb) and Yb_2O_3 Co-doped Y_2O_3 stabilized ZrO_2 ceramics [J]. Ceramics International, 2016, 42(6): 7360−7365.

未热解厚热障涂层的隔热能力和黏接强度

Mohammad IZADINIA[1,2], Reza SOLTANI[1], Mahmoud HEYDARZADEH SOHI[1], Javad MOSTAGHIMI[2]

1. School of Metallurgy and Materials Engineering, College of Engineering, University of Tehran, Tehran, Iran;

2. Centre for Advanced Coating Technologies, Department of Mechanical and Industrial Engineering, University of Toronto, Toronto, Ontario, Canada

摘　要：对比研究使用未热解粉末制备的厚热障涂层(UPTTBC)和传统 TBC、厚 TBC(TTBC)及密集垂直裂纹(DVC)TTBC 4 种涂层的隔热能力和黏接强度。采用降温法测试涂层的隔热能力；根据 ASTM C633 标准，采用拉拔试验检测涂层的黏接强度。结果显示，UPTTBC 和 DVC TTBC 的黏接强度分别比 TTBC 高 35%和 25%。这可能是由于 UPTTBC 结构中存在亚微米尺度的未熔化区域，起到了阻止裂纹扩展的作用。此外，隔热测试的结果表明，DVC TTBC 涂层的隔热能力最差，为 0.28 ℃/μm，而 UPTTBC 涂层的隔热能力最强，为 0.40 ℃/μm。由于 UPTTBCs 显微组织中存在亚微米区域，使涂层展现出优越的隔热能力。相反，DVC TTBC 因其致密的结构，具有最低的隔热能力。

关键词：厚热障涂层；密集垂直裂纹热障涂层；未热解粉末；黏接强度；隔热能力

(Edited by Bing YANG)